International Journal of Current Advanced Research
ISSN: O: 2319-6475, ISSN: P: 2319-6505, Impact Factor: 6.614
Available Online at www.journalijcar.org
Volume 10; Issue 02 (C); February 2021; Page No.23897-23902
DOI: http://dx.doi.org/10.24327/ijcar.2021.23902.4736

Research Article

THERMAL INVESTIGATION OF SPACECRAFT OPTICAL ELECTRONIC OBSERVATION SYSTEM WITHOUT PROTECTIVE COVER IN LOW EARTH ORBIT

Ahmed Farag

Aeronautical Engineering Department, Institute of Aviation Engineering and Technology, Giza, Egypt

ARTICLE INFO

Article History:
Received 10th November, 2020
Received in revised form 2nd December, 2020
Accepted 26th January, 2021
Published online 28th February, 2021

Key words:

Spacecraft, thermal control, external heat fluxes, payload, mirror.

ABSTRACT

The present work was dedicated to the development and introduction of the effect of no payload cover on image quality during spacecraft(SC) operation. Payload is mounted as a monoblock on a framework (constituting the SC body) along +Z axis on the side of upper end panel. The analysis is done for payload configuration with permanently open protective cover. Thermal simulation and payload elements temperature analysis is performed using software Thermal Desktop/Sinda Fluent. The goal of analysis is to determine temperature variation of payload elements (primary mirror, carbon plastic cylinder, light protective tube) in stand-by mode and in session mode under effect of external heat fluxes with electric heaters (EH) automatic operation when maintaining average temperature of the primary mirror at 20°C and given EH arrangement. Required EH power with different EH switching on/off configurations in order to is estimated to maintain the primary mirror temperature at 20°C taking into account allowed number of operation cycles (switching on-off) of switching keys of 90000 over the whole SC lifetime. The analysis is performed with SC moving in Low Earth Orbit (LEO).At that two extreme SC orientation modes with respect to external heat fluxes effect are considered (maximum external heat fluxes, and minimum external heat fluxes).

INTRODUCTION

Thermal control system guarantees all subsystems and equipment to operate within its temperature ranges during SC lifetime. This paper studies the optimum thermal control system design for a payload for SC by performing thermal analysis through special software program. [1].Payload is mounted as a monoblock on a framework (constituting the SC body) along +Z axis on the side of upper end panel. The analysis is done for payload configuration with permanently open protective cover.

Thermal simulation and payload elements temperature analysis is performed using software Thermal Desktop/Sinda Fluent. The goal of analysis is to determine temperature variation of payload elements (primary mirror, carbon plastic cylinder, light protective tube) with SC moving in Low Earth Orbit(LEO) in stand-by mode and in session mode under effect of external heat fluxes with electric heaters (EH) automatic operation when maintaining average temperature of the primary mirror at 20°C and given EH arrangement.

The analysis objectives are

- To determine temperature field over the primary mirror (over the thickness and in radial direction);
- To determine temperature field variation over the base plate;
- To determine temperature field variation over light protective tube
- To estimate required EH power with different EH switching on/off configurations in order to maintain the primary mirror temperature at 20°C taking into account allowed number of operation cycles (switching on-off) of switching keys of 90000 over the whole SC lifetime.

Figure 1 Spacecraft (SC) External View

Governing Equations

The program solves the energy conservation (Heat Rejection Budget) equation under transient conditions [2].The general form is:

Corresponding author:* **Ahmed Farag
Aeronautical Engineering Department, Institute of Aviation Engineering and Technology, Giza, Egypt

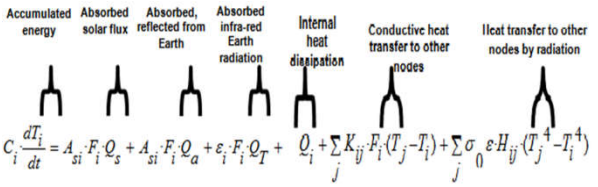

$$C_i \frac{dT_i}{dt} = A_{si} F_i Q_s + A_{si} F_i Q_a + \varepsilon_i F_i Q_T + Q_i + \sum_j K_{ij} F_i (T_j - T_i) + \sum_j \sigma_0 \varepsilon H_{ij} (T_j^4 - T_i^4) \quad (1)$$

$$q_S A_s F_{rad} + q_E \varepsilon F_{rad} + q_{SB} \varepsilon F_{rad} + Q_{diss} - \varepsilon \sigma T^4 F_{rad} = 0 \quad (2)$$

$$q_S = q_{Solar} + q_{Albedo} \quad (3)$$

Calculations of Heaters Power (Q_{Heater}) :[4]

$$Q_{diss\text{-}min} + Q_{Heater} - \varepsilon \sigma T^4 F_{rad} = 0 \quad (4)$$

Where:

Asi Absorptivity factor (node i) [-]
Q_T Earth infra-red [W/m^2]
Fi Area (node i) [m^2]
Q_I Heat rejection (node i) [W/m^2]
Qs Incident sun flux [W/m^2]
Qa Solar albedo [W/m^2]
ei Emissivity factor [-]
Kij Heat transfer by conduction [W/K]
εHij Heat transfer by radiation [m^2]
q_S Incident Solar flux and albedo [W/m^2]
q_E Earth infra-red (IR) [W/m^2]
q_{SB} Solar Cells flux [W/m^2]
C_iThermal capacitance (node i) [J/K]
Q_{diss} Heat rejection from equipment [W]
σ_0 Stefan-Boltzmann constant [=5.67.10^{-8} W/m^2/K^4]

Numerical Simulation

Problem Formulation

SC model in Low Earth Sun-synchronous Orbit, quasi-circular at 700 Km is created by Thermal desktop program. The analysis is done for payload configuration with permanently open protective cover.[5, 6].

Computational Work

Numerical analysis was performed to model the space characteristics. In order to solve the mentioned task Optical Electronic Module(OEM) thermal model has been developed that allow to monitor variation of heat exchange conditions of OEM elements with each other and with environment.

The models includes the following submodels: [7].

- Primary mirror;
- Light protective cylinder;
- Thermal Buffer;
- Baseplate;
- Secondary mirror;
- Carbon plastic cylinder.

Model reference point – at the centre of the base plate on the upper skin. +Z axis - a longitudinal axis of optical system. Geometrical representation of the OEM thermal model is given in fig. 2.

The thermal model simulates

- Radiant coupling – is formed by Software (SW) on the results of computation of angular coefficients and according to given optical characteristics of surfaces;
- External heat fluxes – are computed by SW according to parameters of the SC orbit and altitude.
- Conductive coupling – is formed by SW according to given heat-conductive properties of the computational nodes and is also set manually between submodel nodes and submodels (special couplings);
- Electrical heaters mounted on the light protective cylinder.

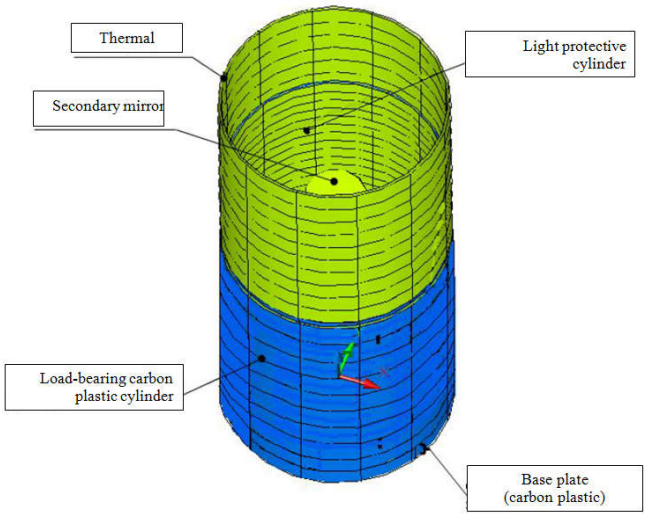

Figure 2 OEM geometrical model

In order to determine angular irradiation coefficients between surfaces of the optical module elements and to determine external heat fluxes (solar and infrared) falling on external surfaces of the module, geometrical submodels of the optical module elements, whose characteristics are given in section 4, were developed beforehand.

Thermal physical properties of materials and optical characteristics of surfaces of optical module elements for determination of radiant couplings, external heat fluxes and conductive couplings are given [7, 8].

Special conductive couplings were simulated in the thermal model for consideration of conductive heat exchange between nodes of submodels. Conductive coupling between the thermal buffer and light protective cylinder is assumed to be 0.2 W/(K·m^2) that corresponds to heat insulation with thermal resistance of 5 (K·m^2)/W.

SC body is not considered in the model and in order to avoid heat exchange with space environment, special optical characteristics of surfaces A_s=0 and ε=0 are set on model's external surfaces structurally located inside SC body.

Boundary Conditions and Analysis Variants

Boundary Conditions

Constant temperature of 20 °C is set on lower (from the side of –Z axis) surface of the base plate in order to simulate space behind the primary mirror (electronic devices of the optical system).All surfaces of the optical system thermal model are located inside the SC body in order to avoid heat exchange with the environment have As=0 and ε=0 [9, 10].

Analysis Variants

The analysis is performed with SC moving in circular orbit at attitude of 698 km. At that two extreme SC orientation modes with respect to external heat fluxes effect are considered:

- Maximum external heat fluxes – OEM flight in the inertial coordinate system (ICS). (-Z axis is pointed to the Sun, X axis coincides with linear velocity vector at orbital noon); during survey OEM is in orbital orientation (OCS) (X axis is pointed in traveling velocity direction, Z axis is pointed to the Earth center), angle between orbital plane and Sun direction β=0°.
- Minimum external heat fluxes – similar to the 1st mode, but angle between orbital plane and Sun direction β=75°, during survey X axis is pointed in traveling velocity direction, Z axis is rolled from the Earth center by 45°; at that during survey the effect of the external heat fluxes jumping on thermal conditions of the primary mirror is determined [11, 12, 13, 14].

External heat fluxes parameters

- Solar constant – 1423 W/(m^2·K);
- Average albedo of the Earth – 0.29.

Analysis variants differ in temperature settings (switching on/off) of EHs in heating belts and groups and SC orientation modes.

Characteristics of analysis variants are given in table 1.

Table 1 Characteristics of analysis variants

Analysis variant number	Electrical heaters operation settings				Angle β
	EH group name		Temperature, C		
			ON	OFF	
1	1st heating belt	main 1	20	26	0°
		main 2	16	22	
		reserve	12	18	
	2nd heating belt	main 1	16	22	
		main 2	12	18	
		reserve	8	14	
2	1st heating belt	main 1	20	26	75° (roll 45°)
		main 2	16	22	
		reserve	12	18	
	2nd heating belt	main 1	16	22	
		main 2	12	18	
		reserve	8	14	

Quasi-stationary temperature values of the model elements in stand-by mode are determined in each variant before the analysis. Survey mode is carried out on three successive revolutions near the sub-solar point.

RESULTS AND DISCUSSIONS

Analysis results are presented as graphs

1. For variant 1 – in figures 6-10;
2. For variant 2 – in figures 11-15;

- Figures present graphs of EH power and temperature of model elements (primary, load-bearing carbon plastic cylinder, light protective tube (1st and 2nd heating belts)) versus time. Graphs are plot according to time 17 revolutions.
- Graphs are plotted for individual model elements:
- For primary mirror – nodes are selected in accordance with figure 3; the graphs present temperature of nodes of external and internal mirror layers;
- For load-bearing carbon plastic cylinder – nodes in four points in height of cylinder are selected in accordance with figure 4;
- For light protective cylinder – nodes representative of the 1st and the 2nd heating belts where EHs (main 1, main 2, reserve) and control TSs are mounted in accordance with figure 5 are selected.

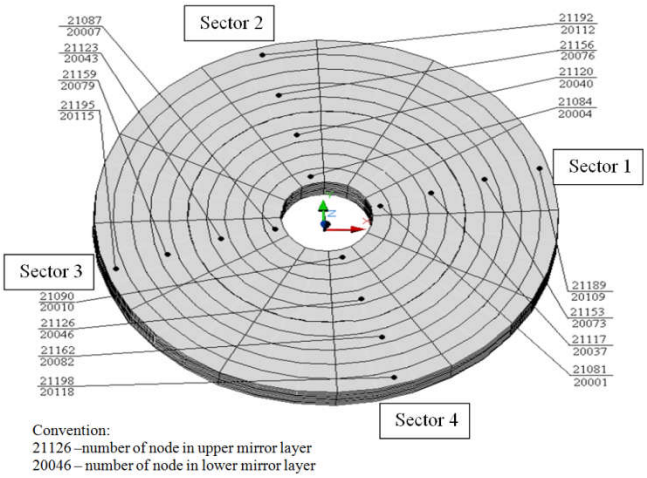

Figure 3 Numbering of the primary mirror nodes

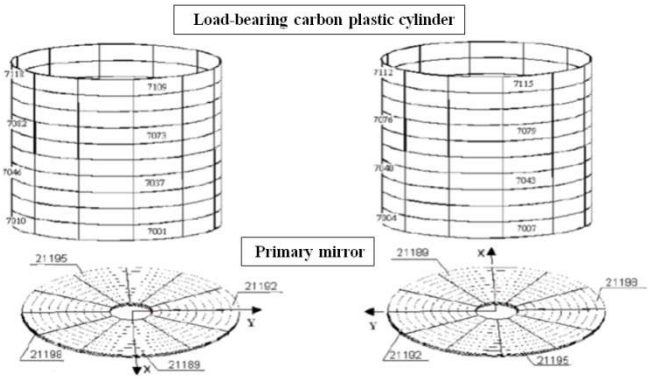

Figure 4 Numbering and location of nodes of load-bearing carbon plastic cylinder whose temperature values are plotted in graphs

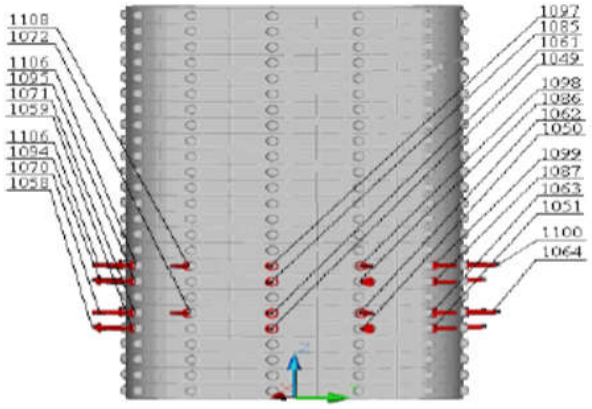

Fig 5 Numbering and location of nodes of light protective cylinder whose temperature values are plotted in graphs

Variant 1

- For days with stand-by revolutions – 56 W;

- For days with three revolutions with survey sessions – 55W;

Variant 2

- For days with stand-by revolutions – 79 W;
- For days with three revolutions with survey sessions – 72 W;
- Maximum limit of EH operation cycles (switching on/off) is:

Variant 1

- For days with stand-by revolutions – 15;
- For days with three revolutions with survey sessions – 14;

Variant 2

- For days with stand-by revolutions – 15;
- For days with three revolutions with survey sessions – 12;

Figure 6 shows the EH operation and its number of cycling (switching ON/OFF), and the relation between the total power consumption with time.

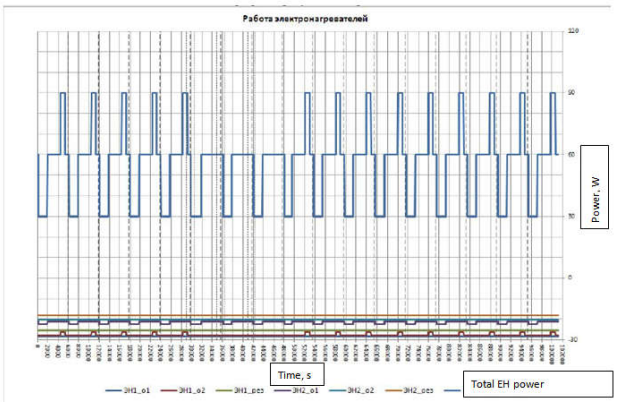

Figure 6 Variant 1. EH operation

Figure 7 shows the relation between the temperatures of the nodes of the primary mirror with time. The temperature of the external layer nodes is higher than temperature of the internal layer nodes, and temperature is in range from 19 to 22 ^{0}C, and it is acceptable along 17 revolutions.

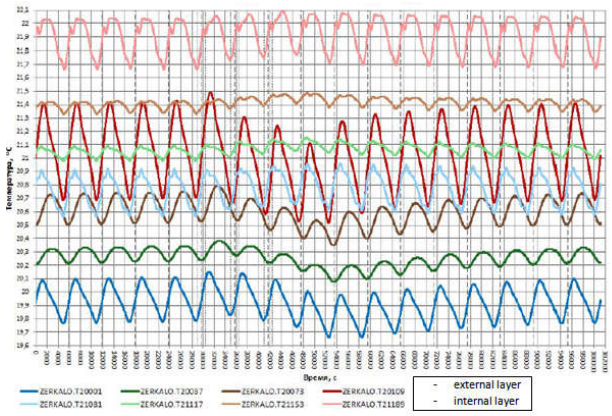

Figure 7 Variant 1. Temperature of the primary mirror nodes (sector 1)

Figure 8 shows the relation between temperature of the load-bearing carbon plastic cylinder and time. The maximum temperature of the nodes is 22 ^{0}C, and it is acceptable along 17 revolutions.

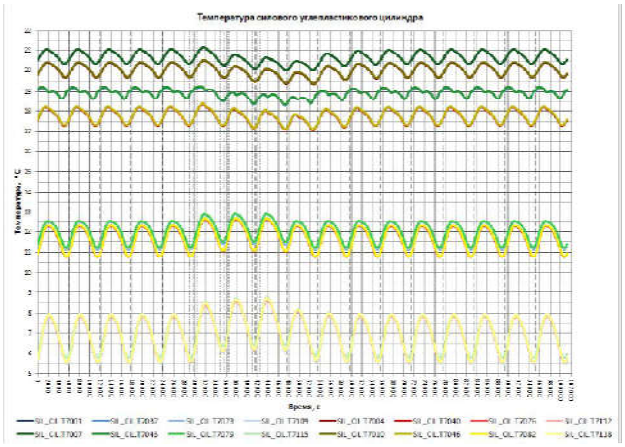

Figure 8 Variant 1. Temperature of the load-bearing carbon plastic cylinder nodes

Figure 9 shows the relation between temperature of the light protective cylinder nodes of the 1st heating belt and time. The maximum temperature of the nodes is 37^{0}C, and it is higher than temperature of the 2nd heating belt because the temperature settings for ON/OFF for each group is higher than the same in 2nd heating belt.

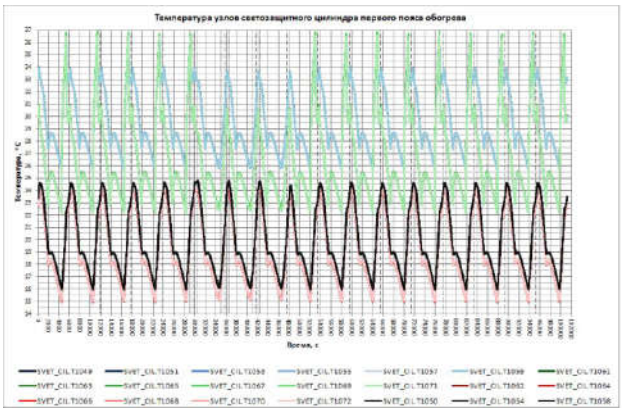

Figure 9 Variant 1. Temperature of the light protective cylinder nodes of the 1st heating belt

Figure 10 shows the relation between temperature of the light protective cylinder nodes of the 2nd heating belt and time. The maximum temperature of the nodes is 32^{0}C, and it is less than temperature of the 1st heating belt because the temperature settings for ON/OFF for each group is less than the same in 1st heating belt.

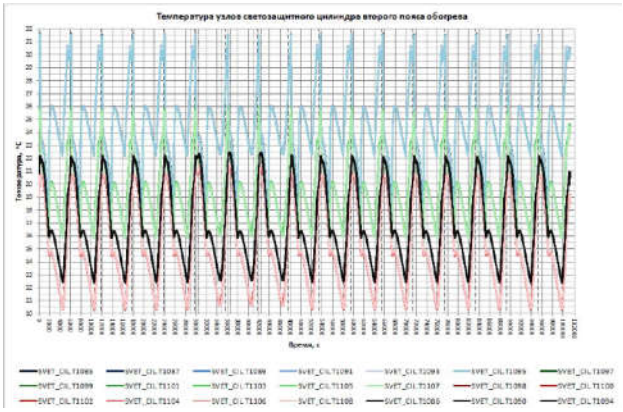

Figure 10 Variant 1. Temperature of the light protective cylinder nodes of the 2nd heating belt

Figure 11 shows the EH operation and its number of cycling (switching ON/OFF),and the relation between the total power consumption with time.

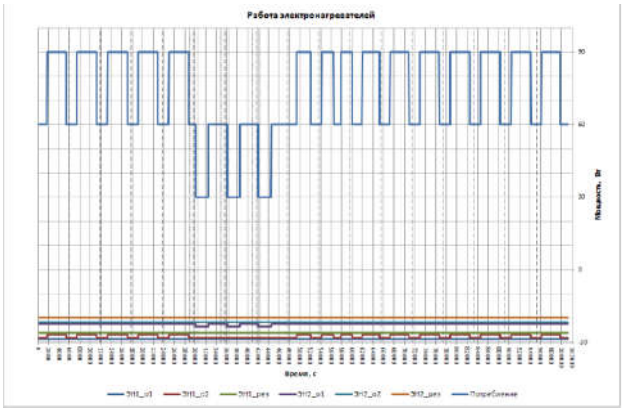

Figure 11 Variant 2. EH operation

Figure 12 shows the relation between the temperatures of the nodes of the primary mirror with time. The temperature of the external layer nodes is higher than temperature of the internal layer nodes, and temperature is in range from 19 to 22 ^{0}C, but it is obvious that during shooting period (3 successive revolutions) the temperature is higher than the other revolutions because EH is ON to support excess heat which is needed for system operation.

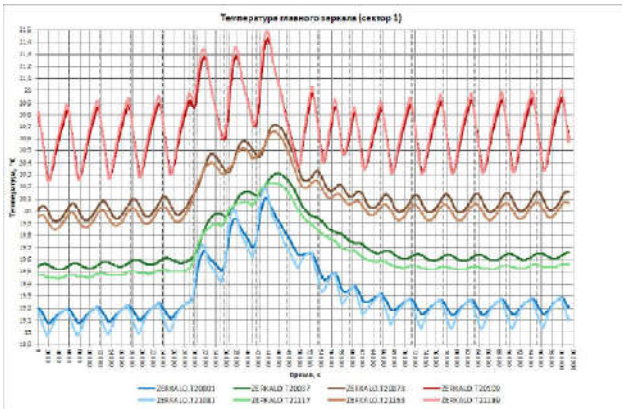

Figure 12 Variant 2. Primary mirror elements temperature (sector 1).

Figure 13 shows the relation between temperature of the load-bearing carbon plastic cylinder and time. The maximum temperature of the nodes is 22 ^{0}C, but it is obvious that during shooting period (3successive revolutions) the temperature is higher than the other revolutions because EH is ON to support excess heat which is needed for system operation.

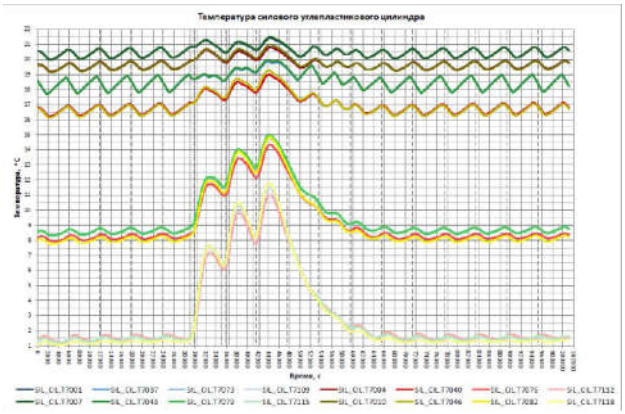

Figure 13 Variant 2. Temperature of the load-bearing carbon plastic cylinder nodes

Figure 14 shows the relation between temperature of the light protective cylinder nodes of the 1st heating belt and time. The maximum temperature of the nodes is 37 ^{0}C, and it is higher than temperature of the 2nd heating belt because the temperature settings for ON/OFF for each group is higher than the same in 2nd heating belt, but it is obvious that during shooting period (3 successive revolutions) the temperature is higher than the other revolutions because EH is ON to support excess heat which is needed for system operation.

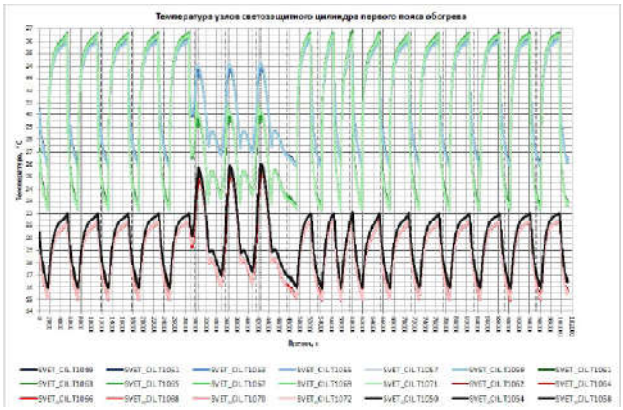

Figure 14 Variant 2. Temperature of the light protective cylinder nodes of the 1st heating belt

Figure 15 shows the relation between temperature of the light protective cylinder nodes of the 2nd heating belt and time. The maximum temperature of the nodes is 32 ^{0}C, and it is less than temperature of the 1st heating belt because the temperature settings for ON/OFF for each group is less than the same in 1st heating belt, but it is obvious that during shooting period (3successive revolutions) the temperature is higher than the other revolutions because EH is ON to support excess heat which is needed for system operation.

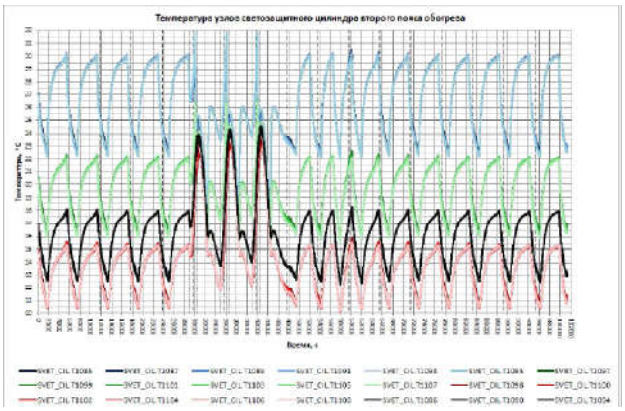

Figure 15 Variant 2. Temperature of the light protective cylinder nodes of the 2nd heating belt

CONCLUSIONS

The most important points in this paper:

- Thermal Desktop Program can create payload model, and calculate temperature field, and power consumption of heaters.
- Analysis performed at the stage of development of work design documentation and confirmed showed the possibility to provide the required OEOS thermal conditions during in-orbit flight with the protective cover permanently open.

- The thermal control system (TCS) with its elements areused to guarantee the specified temperature ranges of all subsystems and equipment during the SC lifetime.

References

1. Gilmore DG. Spacecraft Thermal Control Handbook Volume I : Fundamental Technologies, 2nd Ed, The Aerospace Press, El Segundo, CA, 2002.
2. Katwijk K Van, Laan T Van Der, Stramaccioni D. Mechanical and Thermal Design of XMM, ESA Bulletin No. 100, 1999.
3. Earth albedo and emitted radiation, NASA SP-8067, 1971.
4. Solar Electromagnetic Radiation, NASA SP-8005, 1971.
5. Smith GD. Numerical Solution of Partial Differential Equations, Oxford University Press, Oxford, United Kingdom, 1978.
6. Ferziger JH. Numerical methods for engineering application. New York: John Wiley and Sons; 1981.
7. Cullimore A. Computer code SINDA '85/FLUINT System Improved Numerical Differencing Analyzer and Fluid Integrator, Version 2.3 (Martin Marietta), 1990.
8. Wertz JR. and Larson WJ. Space Mission Analysis and Design, 3rd Ed, Microcosm, 1999.
9. Boulder, CO, Operationally Responsive Space Missions, Master's Thesis, University of Colorado, Department of Aerospace Engineering Sciences, 2005.
10. Wise EC, Raisch J, Kelly W, Sharma SE. Thermal Design Verification of a High Power Direct Broadcast Satellite. AIAA-86-1339 1986.
11. Barton M, Miller J. Thermal Design of a Spacecraft on a Module Level for LEO Missions. 19th Annu AIAA/USU Conf Small Satell 2005:SSC06-III-1.
12. Stanton S, Sellers J. Modeling and simulation tools for rapid space system analysis and design: FalconSat-2 applications. IEEE Aerosp Conf Proc 2001;7:73479–87. doi:10.1109/AERO.2001.931426.
13. Roberto Opromolla *et al*. 2017 "A new star tracker concept for satellite attitude determination based on a multi-purpose panoramic camera".
14. Lin Yang *et al*. 2019 "Quasi-All-Passive Thermal Control System Design and On-Orbit Validation of Luojia 1-01 Satellite".

How to cite this article:

Ahmed Farag (2021) 'Thermal Investigation of Spacecraft Optical Electronic Observation System without Protective Cover in Low Earth Orbit', *International Journal of Current Advanced Research,* 10(02), pp. 23897-23902.
DOI: http://dx.doi.org/10.24327/ijcar.2021. 23902.4736

****